Journal of Alloys and Compounds 509 (2011) 7052–7059

Contents lists available at ScienceDirect

Journal of Alloys and Compounds

journal homepage: www.elsevier.com/locate/jallcom

Kinetics of intermetallic phase formation at the interface of Sn–Ag–Cu–X (X = Bi, In) solders with Cu substrate

Erika Hodúlová[a], Marián Palcut[b,*], Emil Lechovič[a], Beáta Šimeková[a], Koloman Ulrich[a]

[a] Institute of Production Technologies, Faculty of Materials Science and Technology, Slovak University of Technology, 91724 Trnava, Slovakia
[b] Institute of Materials Science, Faculty of Materials Science and Technology, Slovak University of Technology, 91724 Trnava, Slovakia

ARTICLE INFO

Article history:
Received 12 January 2011
Received in revised form 28 March 2011
Accepted 29 March 2011
Available online 5 April 2011

Keywords:
Lead-free solder
Intermetallic compound formation
Diffusion
Kinetics
X-ray spectroscopy

ABSTRACT

The effects of Bi and In additions on intermetallic phase formation in lead-free solder joints of Sn–3.7Ag–0.7Cu; Sn–1.0Ag–0.5Cu–1.0Bi and Sn–1.5Ag–0.7Cu–9.5In (composition given in weight %) with copper substrate are studied. Soldering of copper plate was conducted at 250 °C for 5 s. The joints were subsequently aged at temperatures of 130–170 °C for 2–16 days in a convection oven. The aged interfaces were analyzed by optical microscopy and energy dispersive X-ray spectroscopy (EDX) microanalysis. Two intermetallic layers are observed at the interface – Cu_3Sn and Cu_6Sn_5. Cu_6Sn_5 is formed during soldering. Cu_3Sn is formed during solid state ageing. Bi and In decrease the growth rate of Cu_3Sn since they appear to inhibit tin diffusion through the grain boundaries. Furthermore, indium was found to produce a new phase – $Cu_6(Sn,In)_5$ instead of Cu_6Sn_5, with a higher rate constant. The mechanism of the $Cu_6(Sn,In)_5$ layer growth is discussed and the conclusions for the optimal solder chemical composition are presented.

1. Introduction

Increasing environmental and health concerns about the lead toxicity limit the use of traditional Sn–Pb alloys in soldering technology and stimulate the development of alternative, lead–free solder alloys for electronic applications [1,2]. Among the currently considered compositions, ternary eutectic Sn–Ag–Cu alloys have received a lot of attention due to their increased strength and a lower wetting angle comparing to binary Sn–Ag eutectic alloys [3]. Ag and Cu elements are used in low concentrations and thus, they are not considered to be an environmental hazard. Nevertheless, challenges remain with respect to the relatively high melting point of these alloys (217 °C). The melting point of a traditional Sn–Pb solder is only 183 °C. In order to decrease the melting point of Sn–Ag–Cu alloys, additional elements in low concentrations are needed. Bismuth and indium are potential candidates that may significantly lower the melting of the Sn–Ag–Cu eutectic [4–9]. Furthermore, it was found that the wetting angle between the solder and copper substrate decreases with increasing indium concentration [10]. On the other hand, the joint strength moderately decreases with increasing amount of indium [10].

During soldering, some of the metal substrate is dissolved into the molten solder. As a result, the solder becomes supersaturated with the dissolved metal and a layer of an intermetallic compound is formed at the metal–solder interface. The intermetallic layer continues to grow after solidification due to thermally activated solid state diffusion mechanisms. The formation and growth of intermetallics at the solder/substrate interface affect the solderability and reliability of electronic solder joints [11]. Intermetallic compounds are generally much harder and more brittle than solders and can, therefore, cause brittle fractures at the interface between the solder and the metal substrate [12]. Due to the high concentration of tin, eutectic Sn–Ag–Cu solders form Cu–Sn intermetallic compounds at the copper substrate [13]. Vianco et al. studied the intermetallic compound formation between copper and 95.5Sn–3.9Ag–0.6Cu (composition given in weight %) and found that layers of Cu_3Sn and Cu_6Sn_5 form at the interface [14]. Cu_6Sn_5 layer is formed during soldering and Cu_3Sn forms during solid state ageing between Cu_6Sn_5 and Cu substrate. The layer growth is diffusion-limited and sensitive to the copper concentration in the solder [14]. Higher copper concentration is shown to produce thicker Cu_3Sn layers [14].

The effect of minor Fe, Co and Ni additions (0.03 wt.%) on the reaction between the Sn–Ag–Cu solder and Cu substrate was investigated by Wang et al. [15,16]. In the solid-state ageing study, the authors found that both Cu_6Sn_5 and Cu_3Sn phases formed. However, the addition of Fe, Co and Ni produced a much thinner Cu_3Sn layer. The thickness of Cu_3Sn was only one third of the layer formed between the Cu substrate and Sn–Ag–Cu solder

* Corresponding author. Present address: Centre of Materials Science and Nanotechnology, Department of Chemistry, University of Oslo, P. O. Box 1033 Blindern, NO-0318 Oslo, Norway. Tel.: +47 228 58232.
E-mail addresses: marian.palcut@gmail.com, marian.palcut@smn.uio.no (M. Palcut).

0925-8388/$ – see front matter © 2011 Elsevier B.V. All rights reserved.
doi:10.1016/j.jallcom.2011.03.164

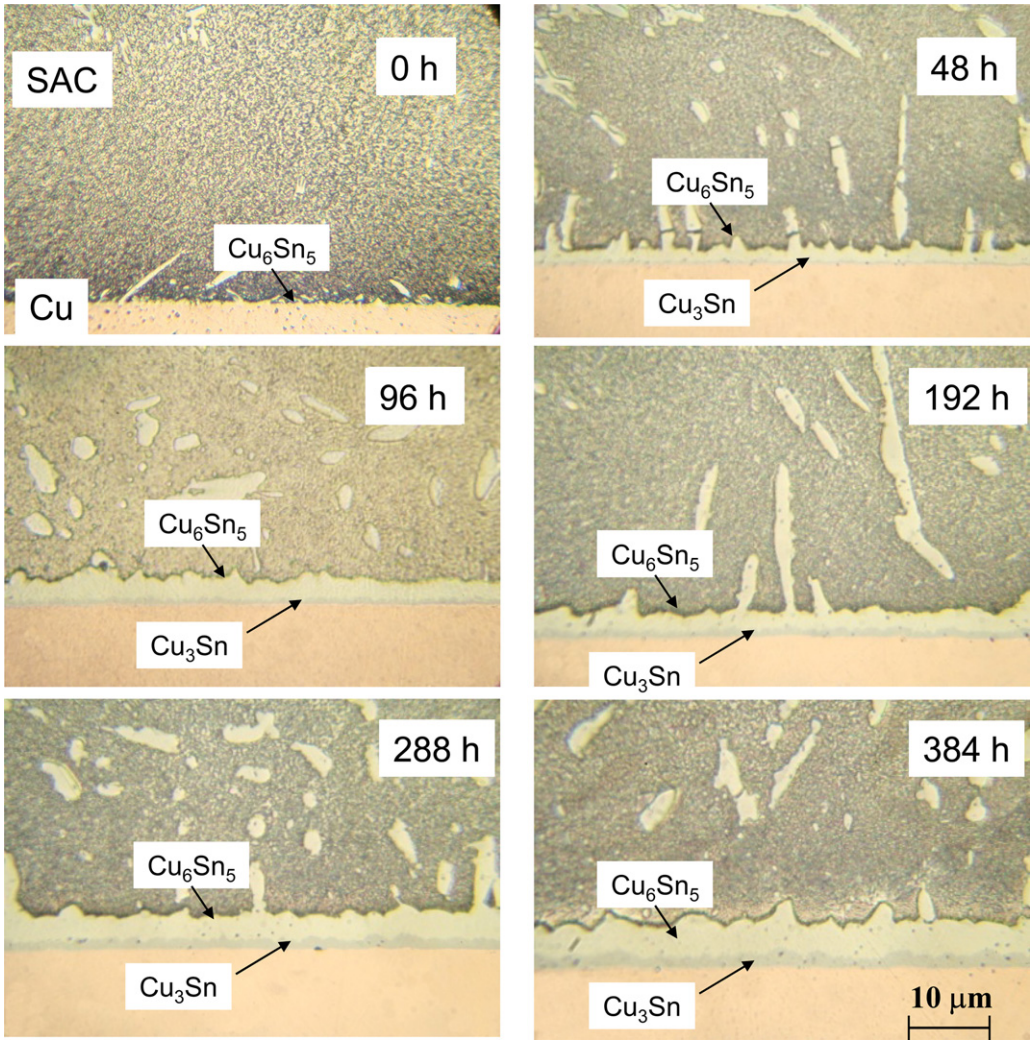

Fig. 1. Microstructure evolution of the Cu/SAC interface after soldering and solid state ageing at 150 °C.

without any additives [15]. Wang et al. observed that Ni additions to lead–free solders produced more of the Cu_6Sn_5 phase during the reflow stage [16]. It was therefore suggested that this thicker Cu_6Sn_5 phase becomes a better diffusion barrier for the Sn atomic flux necessary for the Cu_3Sn growth [16]. Yoon et al. studied the intermetallic growth rate between Sn–Ag–(Cu/Ni) solders and ENIG (electroless nickel–immersion gold) substrates and found that the growth rate was about 3.3 times slower comparing to Cu substrates [17]. The same group studied the sequential intermetallic compound formation of Cu_6Sn_5 and Ni_3Sn_4 between SnAgCu solder and ENEPIG (electroless nickel–electroless palladium–immersion gold) substrate during the reflow process [18]. Initially, a discontinuous polygonal-shape $(Cu,Ni)_6Sn_5$ phase formed at the interface. However, during the reflow process for up to 60 min, a $(Cu,Ni)_3Sn_4$ intermetallic phase appeared and started to grow. At later stages, it embedded the discontinuous $(Cu,Ni)_6Sn_5$ phase [18]. It was suggested that the interfacial product variation resulted from the preferential consumption of Cu within the solder and continuous Ni diffusion from the Ni(P) layer [18].

The interfacial reactions between Sn–Ag–Cu solder with Ni (0.05 wt.%) and Ge (0.01 wt.%) additions and Au/Ni/Cu substrate were studied by Yen et al. [19]. The authors reported that the Ni and Ge additions did not influence the interfacial reaction. However, the Ge aggregation on the solder ball surface was found to enhance the solder's anti-oxidation ability [19]. The effects of Ce and Zn additions on the microstructure and mechanical properties of Sn–Ag–Cu solder joints have recently been investigated by Lin and Chuang [20]. Xue and co-workers studied the effects of rare earth elements on the properties and microstructures of lead–free solders and found that the Cu_6Sn_5 growth rate could be efficiently reduced by adding a trace amount Ce [21]. Therefore, the rare earth elements could be labeled as the "vitamins" of metals [22]. Laurila et al. recently reviewed the impurity and alloying effects on interfacial reaction layers in lead–free soldering [23]. The authors found that the elements may have three major effects:

1. The elements can change the reaction rate between the solder and metal substrate.
2. The additives can alter the physical properties of the intermetallic (IMC) phases formed at the solder–substrate interface.
3. The elements can form additional reaction layers at the interface or they can displace the binary phases that would normally appear and form other reaction products instead.

Furthermore, the alloying element effect was found to depend on their solubility in the IMC layer. The elements that have a marked solubility in the IMC layer have the most pronounced effect on the IMC formation [23].

The influence of dopant on the growth of intermetallic layers in Sn–Ag–Cu solder joints with copper has recently been inves-

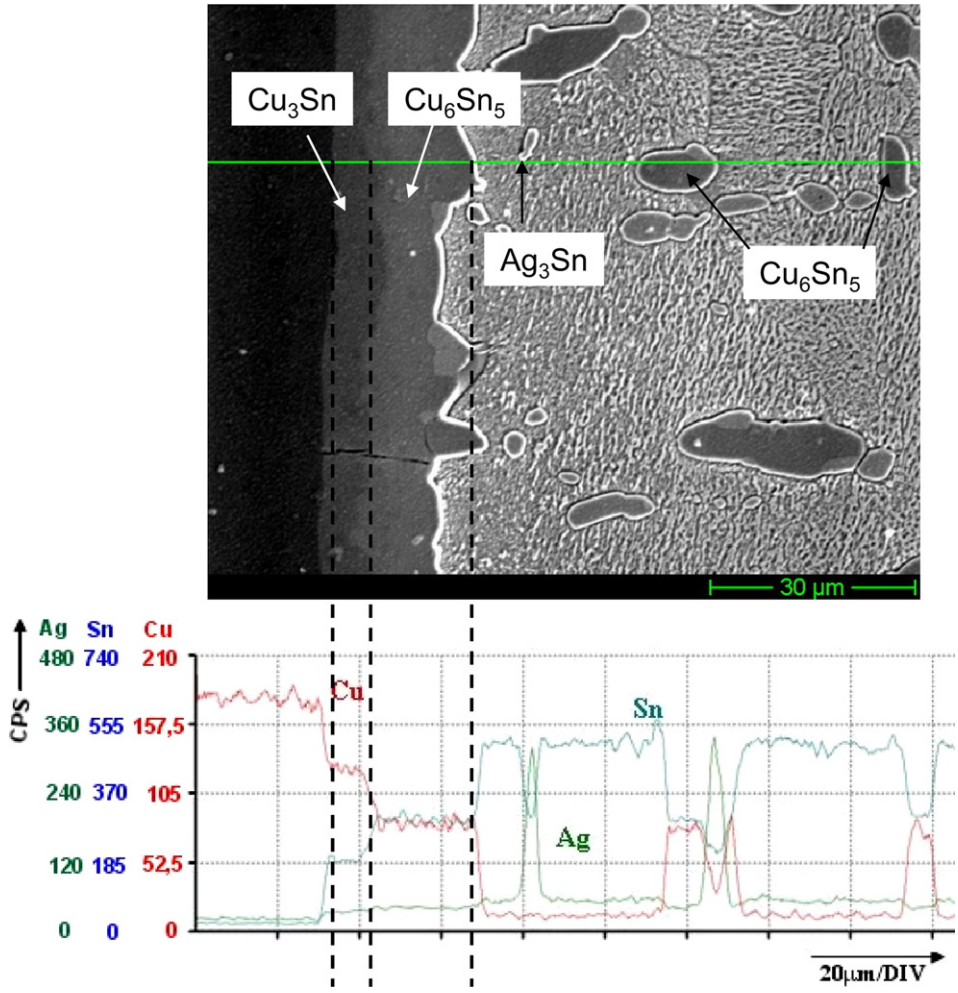

Fig. 2. Element distributions across the Cu/SAC interface, measured by EDX, after solid state ageing for 384 h.

tigated by Li et al. [24] The authors studied the interactions of Sn–3.5Ag–0.7Cu–*x*Sb alloys with different antimony concentrations (0.2–2.0%) [24]. They found that antimony increases the activation energy of Cu_6Sn_5 layer formation, reduces the atomic diffusion rate and thus inhibits the excessive growth of intermetallic compounds. The authors suggested that the effect of Sb additions can be explained by grain boundary obstruction mechanism [24]. Similarly, Rizvi et al. observed a beneficial effect of bismuth additions in Sn–Ag–Cu solder alloy on the decrease of intermetallic layer growth [25]. The authors found that the parabolic rate constant for the intermetallic layer growth decreases from 2.21×10^{-17} m^2 s^{-1} to 1.91×10^{-17} m^2 s^{-1} at 150 °C upon addition of 1% Bi into Sn–2.8Ag–0.5Cu [25]. To the best of our knowledge, the effect of indium on the intermetallic compound formation during solid state ageing at the Cu/Sn–Ag–Cu–In interface has not been investigated yet. The effect of indium is expected to be significant since this element is known to substitute tin in intermetallic compounds [9]. The formation of $Cu_6(Sn,In)_5$ compound has been observed in Cu/In–Sn couples [26]. The substitution of tin may alter the atomic diffusion and growth mechanism of this compound.

In the present work, the kinetics of intermetallic phase formation between Cu substrate and Sn–1.5Ag–0.7Cu–9.5In solder alloy is studied and compared to Sn–Ag–Cu and Sn–Ag–Cu–Bi solders. Sn–1.5Ag–0.7Cu–9.5In alloy is a candidate material for lead–free soldering at temperatures close to 200 °C due to significant amount of indium.

2. Experimental

The lead free solder samples were prepared by melting the pure metals (Sn, Ag, Cu, Bi, In), in the respective concentrations, in alumina crucibles. The metals used were of 99.99% purity. The chemical compositions of the samples, measured by the energy dispersive X-ray spectrometry (EDX, JEOL-JXA-840A), are given in Table 1. Technical copper plate (99.99%) was used as the substrate material. The copper surface was ground, polished with diamond paste (1 μm finish) and cleaned with an ultrasonic cleaner.

The soldering of the copper plate was conducted at 250 °C for 5 s. After soldering, the samples were quenched to room temperature. The joints were subsequently aged at temperatures of 130–170 °C for 2–16 days in a convection oven. The samples were gradually taken from the furnace after 2, 4, 8, 12 and 16 days. The samples were mounted in epoxy resin and cross sections were made. Prior to the analysis, the interface was polished with diamond paste and etched in a nitric acid solution (5% HNO_3 + 2% HCl + 93% methanol) for 2–4 s. The microstructure of the soldered joints and the morphology of intermetallic phases were investigated by the optical microscope. The intermetallic phases were analyzed by the image analysis software. By using the software it was possible to calculate the area occupied by each phase. The mean layer thickness was then calculated by dividing the total phase area by the image length. The chemical composition of the phases was investigated by EDX microanalysis (JEOL-JXA-840A). The results are presented below.

Table 1
Chemical composition (in weight %) of the investigated solders.

Acronym	Sn	Ag	Cu	Bi	In
SAC	95.6	3.7	0.7	–	–
SACB	97.5	1.0	0.5	1.0	–
SACI	88.7	1.5	0.7	–	9.5

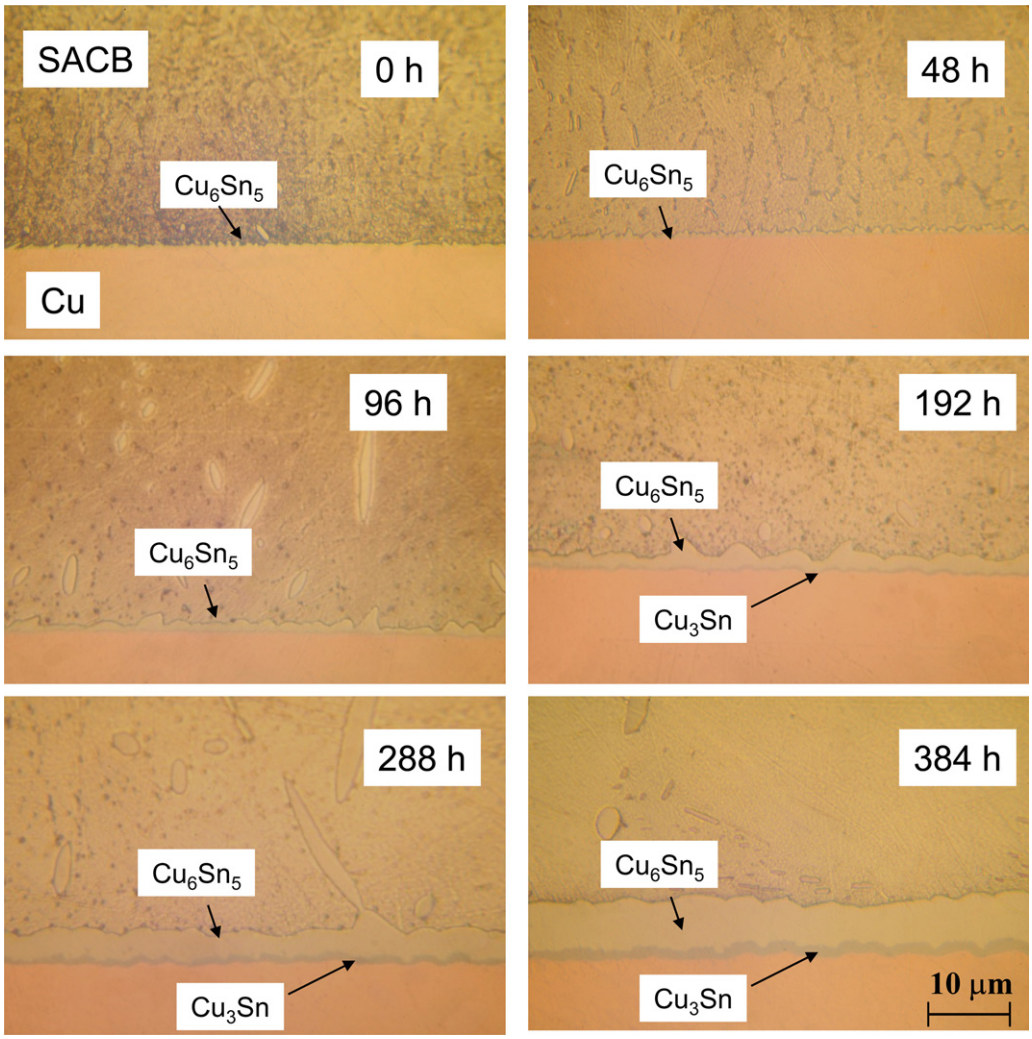

Fig. 3. Microstructure evolution of the Cu/SACB interface after soldering and solid state ageing at 150 °C.

3. Results

The microstructure of the Sn–Ag–Cu(SAC) solder joint with Cu substrate is presented in Fig. 1. Immediately after soldering, the interface layer between the materials consisted of a scallop-shaped Cu_6Sn_5, with an average thickness of 1.2 μm. During the subsequent solid-state ageing, this layer continued to grow. Moreover, a continuous Cu_3Sn layer appeared and started to grow between the copper substrate and Cu_6Sn_5. The chemical composition of the cross section is presented in Fig. 2. It is possible to observe that besides the Cu_6Sn_5 and Cu_3Sn layers located at the interface, there are also isolated intermetallic phase precipitates located inside the solder bulk (Ag_3Sn, Cu_6Sn_5).

The microstructure of the Sn–Ag–Cu–Bi(SACB) solder joint with Cu substrate is presented in Fig. 3. Similarly to the previous case, the interface layer between the materials immediately after the soldering consisted only of a scallop-shaped Cu_6Sn_5. The average thickness of Cu_6Sn_5 was 0.85 μm. During the subsequent solid-state ageing, this layer continued to grow. Cu_6Sn_5 layer is formed by nucleation during soldering between the solid copper substrate and liquid Sn-based lead free solder. At early stages, the layer is expected to grow in the horizontal direction until the grains start impinging one another. The scallop-like shape of this phase is probably a result of the grain coarsening. The scallop-like shape disappears at later stages of ageing which suggests a change in the growth mechanism to the steady growth in the perpendicular direction to the interface. The chemical composition of the cross section is presented in Fig. 4. Bismuth does not significantly influence the chemical composition of intermetallic phases. This is probably due to the low concentration. The element is located mostly in the solder bulk. Nevertheless, bismuth seems to suppress the formation of the second layer, Cu_3Sn. The thickness is smaller comparing to the Cu_3Sn layer formed at the Cu–SAC interface. Table 2 provides the Cu_3Sn layer thickness for each solder composition.

Fig. 5 shows the microstructure of the Sn–Ag–Cu–In(SACI) solder joint with Cu substrate. The interface layer consists of the $Cu_6(Sn,In)_5$ mostly, with a considerable amount of tin substituted by indium. The Cu_3Sn layer is discontinuous and its

Table 2
Thickness of the Cu_3Sn layer in the SAC–Cu, SACB–Cu and SACI–Cu solder joints at 423 K.

t/h	SAC–Cu	SACB–Cu	SACI–Cu
0	0	0	0
48	0.88	0.52	1.07
96	1.24	0.9	1.16
192	1.45	1.29	1.66
288	2.72	2.33	1.86
384	3.25	2.75	1.96

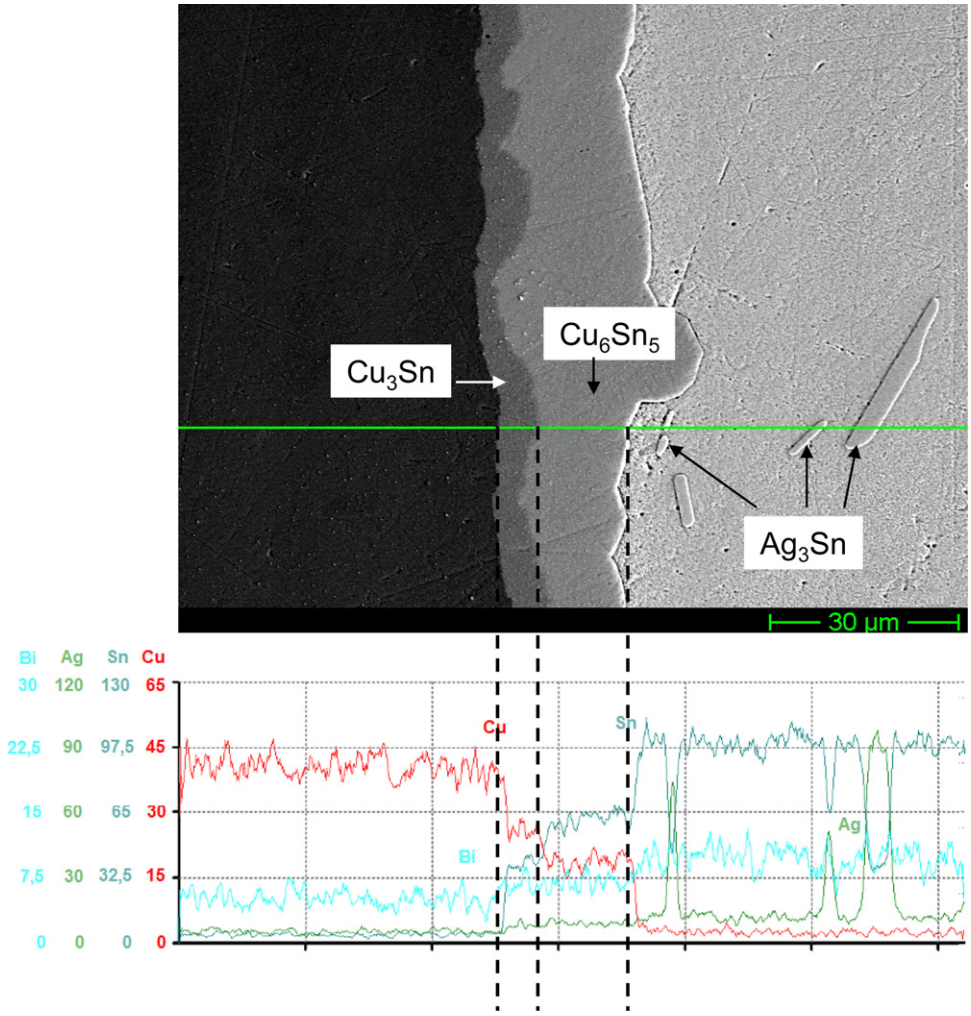

Fig. 4. Element distributions across the Cu/SACB interface, measured by EDX, after solid state ageing for 384 h.

thickness is small compared to the previous samples after 16 days of ageing. The chemical composition of intermetallic layers is given in Fig. 6. A significant amount of indium is present in all phases, except Cu_3Sn. Indium concentration in the Ag_3Sn is much higher comparing to other intermetallics. This is probably due to the partial transformation of this phase into Ag_2In [7,9]. The time evolution of the $Cu_6(Sn,In)_5$ layer thickness is given in Fig. 7. The $Cu_6(Sn,In)_5$ layer grows with a significantly higher rate comparing to Cu_6Sn_5. The formation of Cu_3Sn is significantly suppressed.

The kinetics of the $Cu_6(Sn,In)_5$ layer formation at three different temperatures is given in Fig. 8. The layer growth follows the parabolic rate law

$$x^2 = k_p t + x_0^2 \quad (1)$$

In this equation x is the layer thickness, t is the ageing time, k_p is the parabolic rate constant and x_0 is the layer thickness before ageing (at $t = 0$ h). The experimental parabolic rate constants are given in Table 3.

Table 3
Rate constants and parameters E_A and A in the Arrhenius equation for intermetallic compound formation at the solder–copper interface. The last two entries are diffusion coefficients of Cu and Sn in Cu_6Sn_5.

		k_p ($m^2\,s^{-1}$)			E_A (kJ mol^{-1})	A ($m^2\,s^{-1}$)	Reference
		130 °C	150 °C	170 °C			
SACI/Cu	$Cu_6(Sn,In)_5$	4.21×10^{-16}	1.25×10^{-15}	2.83×10^{-15}	70.9	6.58×10^{-7}	Present data
SAC/Cu	Cu_6Sn_5		2.97×10^{-16}				Present data
SACB/Cu	Cu_6Sn_5		1.91×10^{-16}				Present data
SAC/Cu	Cu_6Sn_5	4.04×10^{-17}	1.61×10^{-16}	2.41×10^{-16}	64.8	1.55×10^{-8}	[16]
SAC/Cu	Cu_6Sn_5	1.32×10^{-16}	4.19×10^{-16}	5.85×10^{-16}	53.92	1.84×10^{-9}	[15]
SAC/Cu	Cu_6Sn_5	8.41×10^{-19}	2.99×10^{-18}	5.69×10^{-18}	69.42	1.32×10^{-9}	[14]
SAC/Cu	Cu_6Sn_5		2.21×10^{-17}				[19]
SACB/Cu	Cu_6Sn_5		1.91×10^{-17}				[19]
Cu	Cu_6Sn_5		7.04×10^{-16}				[21]
Sn	Cu_6Sn_5		6.49×10^{-16}				[21]

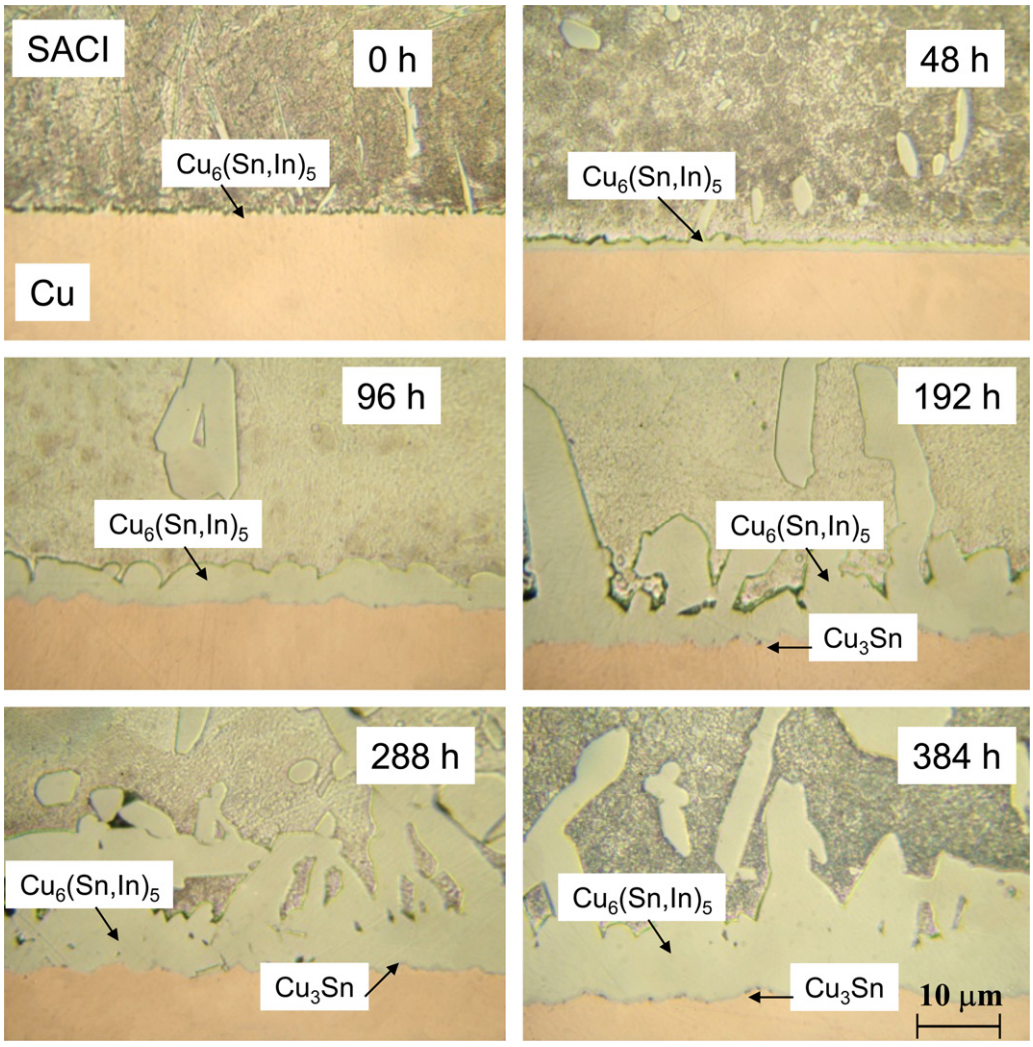

Fig. 5. Microstructure evolution of the Cu/SACI interface after soldering and solid state ageing at 150 °C.

The growth kinetics is thermally activated (Fig. 9). The parabolic rate constants obey the Arrhenius equation

$$\log k_p = \log A - 0.434\frac{E_A}{RT} \quad (2)$$

In this equation, A is the pre-exponential factor, E_A is the activation energy, R is the molar gas constant and T is the ageing temperature. The apparent activation energy for the $Cu_6(Sn,In)_5$ layer formation is 70.9 kJ mol^{-1}.

4. Discussion

Bismuth decreases the rate of Cu_3Sn layer formation (Table 2). The effect of indium on the intermetallic layer formation is two-fold:

1. It decreases the rate of Cu_3Sn layer formation after 288 h;
2. It increases the rate of $Cu_6(Sn,In)_5$ layer formation.

Indium has not been observed in Cu_3Sn (Fig. 6). However, since it is very difficult to measure the Cu_3Sn chemical composition due to the very small layer thickness, it cannot be concluded that indium does not substitute tin in this compound. The formation of indium-substituted $Cu_3(Sn,In)$ has been observed during In–49Sn/Cu soldering reactions [26]. It is, therefore, probable that some tin was substituted by indium also in this compound. Since Cu_3Sn layer is located between Cu and Cu_6Sn_5, two growth mechanisms are possible. At the Cu/Cu_3Sn interface, the layer grows due to the reaction between Cu and diffused Sn according to the following equation

$$3Cu + Sn = Cu_3Sn \quad (3)$$

At the Cu_6Sn_5/Cu_3Sn interface, the layer grows due to interaction between Cu_6Sn_5 with diffused Cu

$$Cu_6Sn_5 + 9Cu = 5Cu_3Sn \quad (4)$$

The relative ratio of Cu and Sn diffusivities in Cu_3Sn determines whether mechanism (3) or (4) dominates. Chao et al. found that Cu diffusivity in Cu_3Sn is about ten times less than Sn diffusivity at 150 °C [27]. This suggests that Cu_3Sn layer formation is given by Sn diffusion and the layer grows at the Cu/Cu_3Sn interface. Wenming et al. recently observed the formation of Kirkendal voids at the Cu/Cu_3Sn interface [28]. This observation suggests that the layer may grow by copper diffusion instead. On the other hand, Laurila et al. did not observe any voids for high purity copper soldered with pure Sn or Sn–Ag–Cu but they did observe them for electrolytic and electroless deposited copper with both Sn and Sn–Ag–Cu alloys [29]. This indicates that the voids are not formed due to the Kirkendall effect but rather due to the redistribution of impurities or volume changes upon formation of intermetallic compounds. Wen-Ming et al. used electrodeposited Cu substrate which might have influenced the void formation [28]. We did not observe any void

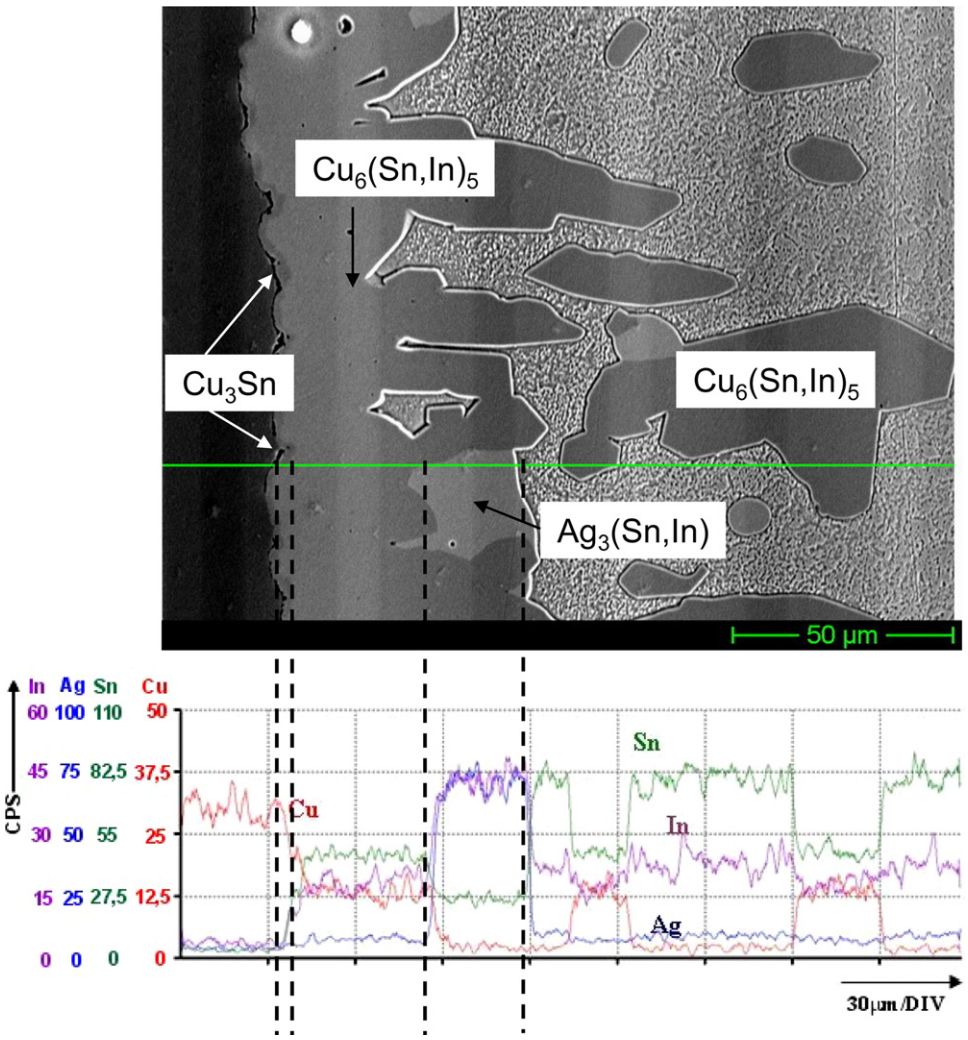

Fig. 6. Element distributions across the Cu/SACI interface, measured by EDX, after solid state ageing for 384 h.

formation in our samples and we used high purity Cu substrate (99.99%).

Based on the previous discussion, it can reasonably be suggested that the Cu_3Sn layer formation is limited by Sn diffusion. Generally, elements diffuse through grain boundaries more rapidly than through the grain interior. A sufficient flux of Sn is needed to maintain the Cu_3Sn growth. Li et al. suggested that, in Sb-doped samples, antimony can substitute tin and form $Cu_3(Sn,Sb)$ particles at grain boundaries of Cu_3Sn [24]. These particles may obstruct the tin diffusion in Cu_3Sn which may lead to the lower growth rate. A similar explanation is possible for solder samples containing Bi and In.

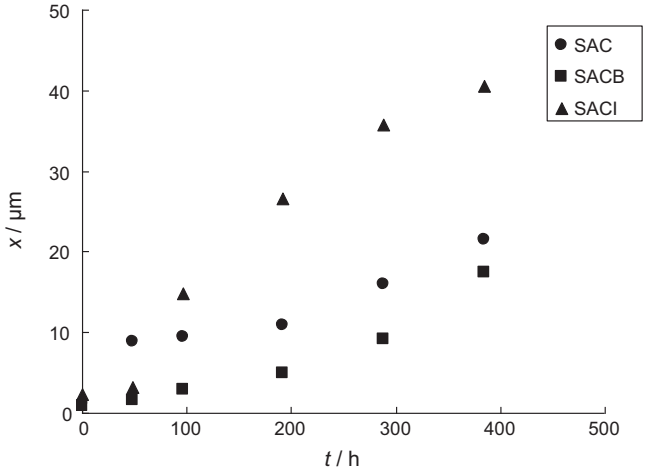

Fig. 7. Thickness of the Cu_6Sn_5 layer ($Cu_6(Sn,In)_5$ for SACI) versus ageing time for the three investigated solder systems at 423 K in air.

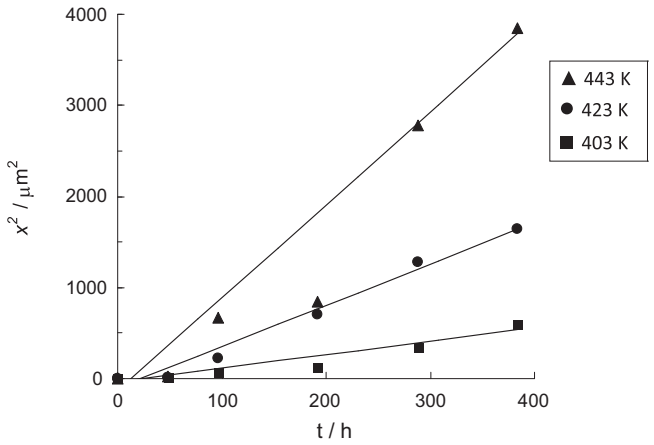

Fig. 8. Parabolic plot of the $Cu_6(Sn,In)_5$ layer thickness versus time for the Cu/SACI interface.

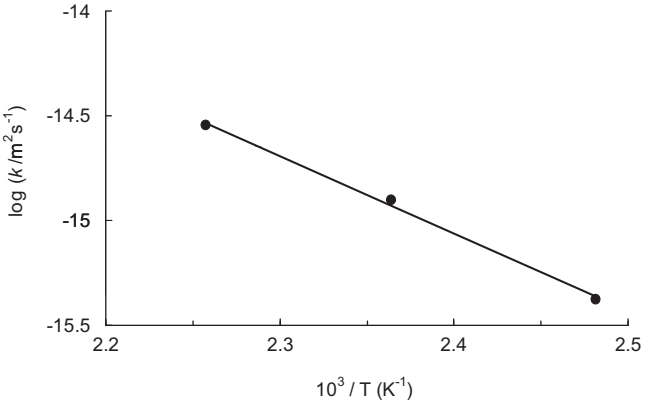

Fig. 9. Arrhenius plot of the parabolic rate constant for the $Cu_6(Sn,In)_5$ layer growth at the SACI–Cu interface.

Since indium has a comparable atomic diameter to tin, it might have a greater tendency to substitute tin in intermetallic compounds, especially at high concentrations. Therefore, the retardation effect could be more pronounced for indium-containing solder compounds comparing to bismuth-doped samples. Nevertheless, the Bi effect is also significant. It has already been shown that 1% Bi may lead to an approximately 10% decrease in the rate constant [25]. The reduction of the intermetallic rate growth decreases the rate of joint degradation and increases the durability.

The observed obedience to the parabolic rate law indicates that the $Cu_6(Sn,In)_5$ layer formation is diffusion-limited (Fig. 8). The diffusion coefficients of Sn and Cu in Cu_6Sn_5 at 150 °C are comparable. This observation suggests that the Cu_6Sn_5 layer probably grows by counter-diffusion of Sn and Cu. Table 3 compares the parabolic rate constants from the present study with the rate constants for the Cu_6Sn_5 growth studied previously. The activation energies are comparable, with only a slightly higher value for $Cu_6(Sn,In)_5$. This suggests that the growth mechanism, i.e., the counter-diffusion of Sn and Cu, is probably maintained. However, the parabolic rate constants for the $Cu_6(Sn,In)_5$ formation are higher, which can be speculated to be due to higher amount of point defects in $Cu_6(Sn,In)_5$. We have previously investigated the composition of the $Cu_6(Sn,In)_5$ phase formed by the solidification of the Sn–1.5Ag–0.7Cu–9.5In alloy [9]. It has been found that the ratio of Cu:(Sn,In) is close to 1 rather than 6:5. This suggests that the crystal structure is probably defective, with some copper atoms missing. Therefore, indium can be suggested to increase copper diffusion. This suggestion is in line with observations of Šebo et al. who studied the indium effect on the microstructure of the interface between Sn–3.13Ag–0.74Cu–xIn and Cu [30]. The authors found that for all indium concentrations studied (4–75%) the phase formed at the solder–substrate interface was copper-rich. Indium increases copper diffusion and leads to the formation of In-based phases at the solder–copper interface. Intermetallic phase precipitates with the $Cu_6(Sn,In)_5$ composition are also formed in the solder bulk (Fig. 5). These phases could reinforce the solder joint. However, they seem to grow rapidly and join the $Cu_6(Sn,In)_5$ phase formed at the interface. The chemical composition of these precipitates is probably not constant. Therefore, further concentration gradients in the layer develop. They, in turn, may increase the copper diffusion and the growth of the layer at later stages of ageing. The excessive intermetallic phase formation may lead to a premature degradation of the working solder joint (Fig. 6).

5. Conclusions

The effect of bismuth and indium in Sn–Ag–Cu solders on the kinetics of intermetallic phase formation at the solder–copper interfaces was investigated. The interface layer consisted of two parallel layers – Cu_3Sn and Cu_6Sn_5. Cu_6Sn_5 was formed during soldering and grew parabolically during subsequent solid state ageing. Cu_3Sn was formed during solid state ageing and its growth rate was decreased by Bi and In additions in the lead-free solder. It is suggested that Cu_3Sn grows by Sn diffusion. Since indium and possibly also bismuth can substitute Sn in intermetallic compounds, $Cu_3(Sn,In)$ or $Cu_3(Sn,Bi)$ compounds may form at Cu_3Sn grain boundaries where they inhibit Sn diffusion.

The parabolic rate constant of the intermetallic layer formation is increased and some tin is substituted by indium in Cu_6Sn_5 at the Cu/Sn–Ag–Cu–In solder joint interfaces. It is suggested that indium increases copper diffusion in $Cu_6(Sn,In)_5$ and leads to the formation of In-based compounds at high concentrations. At later stages of ageing, the $Cu_6(Sn,In)_5$ layer growth is further enhanced by intermetallic phase precipitation in the solder bulk, which may lead to a pre-mature degradation of the solder joint. The indium concentration should, therefore, be lowered to avoid the excessive precipitation of $Cu_6(Sn,In)_5$ in the bulk.

Acknowledgements

Prof. Ján Lokaj is acknowledged for EDX measurements. Prof. Milan Ožvold and prof. Milan Turňa are thanked for their useful comments and suggestions during the project. Dr David S. Wragg is thanked for the English language polishing. This work was supported by grants VEGA 1/0111/10 and VEGA 1/0339/11 of the Ministry of Education, Science, Research and Sport of the Slovak Republic.

References

[1] K. Suganuma, Curr. Opin. Solid State Mater. Sci. 5 (2001) 55.
[2] S. Herat, Clean 36 (2008) 145.
[3] M.E. Loomans, M.E. Fine, Metall. Mater. Trans. A 31 (2000) 1155.
[4] S.-W. Chen, C.-H. Wang, S.-K. Lin, C.-N. Chiu, J. Mater. Sci.: Mater. Electron. 18 (2007) 19.
[5] I. Ohnuma, M. Miyashita, K. Anzai, X.J. Liu, H. Ohtani, R. Kainuma, K. Ishida, J. Electron. Mater. 29 (2000) 1137.
[6] X.J. Liu, Y. Inohana, Y. Takaku, I. Ohnuma, R. Kainuma, K. Ishida, Z. Moser, W. Gasior, J. Pstrus, J. Electron. Mater. 31 (2002) 1139.
[7] L. Gao, S. Xue, L. Zhang, Z. Sheng, F. Ji, W. Dai, S.-L. Yu, G. Zeng, Microelectron. Eng. 87 (2010) 2025.
[8] M. Palcut, J. Sopoušek, L. Trnková, E. Hodúlová, B. Szewczyková, M. Ožvold, M. Turňa, J. Janovec, Kovove Mater. 47 (2009) 43.
[9] J. Sopoušek, M. Palcut, E. Hodúlová, J. Janovec, J. Electron. Mater. 39 (2010) 312.
[10] P. Šebo, P. Štefánik, Kovove Mater. 43 (2005) 202.
[11] Y. Wu, J.A. Sees, C. Pouraghabagher, L.A. Foster, J.L. Marshall, E.G. Jacobs, R.F. Pinizzotto, J. Electron. Mater. 22 (1993) 769.
[12] P.E. Tegehall, Review of the impact of intermetallic layers on the brittleness of tin.lead and lead-free solder joints, IVF project report 06/07, IVF Industrial Research and Development Corporation, Mölndal, Sweden, 2006.
[13] Y.M. Kim, H.-R. Roh, S. Kim, Y.-H. Kim, J. Electron. Mater. 39 (2010) 2504.
[14] P.T. Vianco, J.A. Rejent, P.F. Hlava, J. Electron. Mater. 33 (2004) 991.
[15] Y.W. Wang, Y.W. Lin, C.T. Tu, C.R. Kao, J. Alloys Compd. 478 (2009) 121.
[16] Y.W. Wang, C.C. Chang, W.M. Chen, C.R. Kao, J. Electron. Mater. 39 (2010) 2636.
[17] J.-W. Yoon, B.-I. Noh, S.-B. Jung, J. Alloys Compd. 506 (2010) 331.
[18] J.-W. Yoon, B.-I. Noh, J.-H. Yoon, H.-B. Kang, S.-B. Jung, J. Alloys Compd. 509 (2011) L153.
[19] Y.-W. Yen, Y.-C. Chiang, C.-C. Jao, D.-W. Liaw, S.-C. Lo, C. Lee, J. Alloys Compd. 509 (2011) 4595.
[20] H.-J. Lin, T.-H. Chuang, J. Alloys Compd. 500 (2010) 167.
[21] L. Zhang, S. Xue, L. Gao, G. Zeng, Z. Sheng, Y. Chen, S. Yu, J. Mater. Sci. Mater. Electron. 20 (2009) 685.
[22] G. Zeng, S. Xue, L. Zhang, L. Gao, W. Dai, J. Luo, J. Mater. Sci. Mater. Electron. 21 (2010) 421.
[23] T. Laurila, V. Vuorinen, M. Paulasto- Kröckel, Mater. Sci. Eng. R 68 (2010) 1.
[24] G.Y. Li, X.D. Bi, Q. Chen, X.Q. Shi, J. Electron. Mater. 40 (2011) 165.
[25] M.J. Rizvi, Y.C. Chan, C. Bailey, H. Lu, M.N. Islam, J. Alloys Compd. 407 (2006) 208.
[26] T.H. Chuang, C.L. Yu, S.Y. Chang, S.S. Wang, J. Electron. Mater. 31 (2002) 640.
[27] B. Chao, S.-H. Chae, X. Zhang, K.-H. Lu, J. Im, P.S. Ho, Acta Mater. 55 (2007) 2805.
[28] T. Wen-ming, H. An-qiang, D.G. Ivey, Trans. Nonferrous Met. Soc. China 20 (2010) 90.
[29] T. Laurila, V. Vuorinen, J.K. Kivilahti, Mater. Sci. Eng. R 49 (2005) 1.
[30] P. Šebo, Z. Moser, P. Švec, D. Janičkovič, E. Dobročka, W. Gasior, J. Pstruś, J. Alloys Compd. 480 (2009) 409.